Available online at www.sciencedirect.com

Resuscitation

journal homepage: www.elsevier.com/locate/resuscitation

Clinical paper

Prognostic value of phase information of 2D T2*-weighted gradient echo brain imaging in cardiac arrest survivors: A preliminary study

Jinhee Jang[a], *Sang Hoon Oh*[b,*], *Yoonho Nam*[a], *Kijeong Lee*[c], *Hyun Seok Choi*[a], *So-Lyung Jung*[a], *Kook-Jin Ahn*[a], *Kyu Nam Park*[b], *Bum-soo Kim*[a]

[a] *Department of Radiology, Seoul St. Mary's Hospital, College of Medicine, The Catholic University of Korea, Seoul, Republic of Korea*
[b] *Department of Emergency Medicine, Seoul St. Mary's Hospital, College of Medicine, The Catholic University of Korea, Seoul, Republic of Korea*
[c] *Department of Neurology, Seoul St. Mary's Hospital, College of Medicine, The Catholic University of Korea, Seoul, Republic of Korea*

Abstract

Background: Predicting neurological outcomes after cardiac arrest is important to guide therapeutic decisions. We assessed the prognostic value of phase information of 2D T2*-weighted gradient echo imaging (T2*WI) of the brain in CA survivors.

Methods: This study included cardiac arrest survivors who had undergone MRI for prognostication. After application of homodyne filtering to T2*WI phase images, the contrast of three venous structures was assessed as normal (score 0) or abnormal (score 1): the superior sagittal sinus, the cortical veins, and the thalamostriate veins. The scores were summarized into a gradient-recalled echo (GRE) summary score. The prognostic performances of T2*WI, diffusion-weighted imaging (DWI), electroencephalography and serum biomarkers were evaluated using receiver operating characteristic (ROC) curves.

Results: Of the 39 enrolled patients, 12 (31%) had good outcomes and 27 (69%) had poor outcomes. ROC curve analysis showed that T2*WI had good prognostic performance; the area under the curve (AUC) of the GRE summary score (0.980, 95% confidence interval CI 0.950–1.000) was comparable to those of conventional outcome predictors, including DWI patterns (0.949, 95% CI 0.889–1.000). The AUC increased when the summary GRE score was added to DWI patterns (0.991, 95% CI 0.973–1.000), although the difference was not statistically significant ($P = 0.117$). Most subjects with isoelectric electroencephalography (5/6) showed abnormally high phase contrast in the cerebral veins.

Conclusions: Filtered phase images of T2*WI showed good prognostic value and can reveal various features of the cerebral metabolic consequences of cardiac arrest, such as decreased neuronal activity and brain death-like patterns.

Keywords: Cardiac arrest, Cardiopulmonary resuscitation, Magnetic resonance imaging (MRI), Prognosis

Introduction

Modern treatments such as therapeutic hypothermia (TH) have improved the neurological outcomes of comatose cardiac arrest (CA) survivors. However, prognostication in such patients has become increasingly complex and continues to pose a challenge.[1] Recently, neurological examination, electrophysiological activity monitoring and biochemical markers have been explored for the prediction of neurological outcomes in these patients.[1,2] Because the brain is highly sensitive to the hypoxia that accompanies CA,[2] magnetic resonance imaging (MRI) of the brain, such as diffusion-weighted imaging (DWI), can reveal the extent of the damage and serve as a promising prognostic method.[3,4]

* Corresponding author at: Department of Emergency Medicine, Seoul St. Mary's Hospital, College of Medicine, The Catholic University of Korea, 222 Banpo-daero, Seocho-gu, Seoul, Republic of Korea.
E-mail address: ohmytweety@catholic.ac.kr (S.H. Oh).

https://doi.org/10.1016/j.resuscitation.2019.05.026
Received 4 March 2019; Received in revised form 20 May 2019; Accepted 23 May 2019

Because the brain relies mainly on aerobic metabolism, assessment of cerebral oxygen metabolism may be useful to estimate neurological damage and for prognostication in CA patients.[5–9] A study evaluated cerebral oxygen metabolism in CA survivors using $^{15}O_2$ positron emission tomography (PET) and reported abnormal oxygen metabolism and its prognostic value in these patients.[5] While a few subsequent studies suggested the value of oxygen metabolism for prognostication in CA survivors,[6–9] the clinical availability of $^{15}O_2$ PET remains limited. Recent studies have suggested the clinical value of the MR-based method to assess cerebral oxygen metabolism,[10,11] which is based on the phase contrast of gradient echo imaging (GRE). Estimated oxygen metabolism parameters from these GRE-based methods were comparable to reference standard $^{15}O_2$ PET measures.[12] However, while MR imaging is substantially more clinically available than $^{15}O_2$ PET, complicated and delicate pulse sequences with relatively long scan times may not be suitable for CA survivors.[13–15]

Two-dimensional T2*-weighted GRE (T2*WI) is a simple MRI technique and is widely used in neuroimaging because of its very short acquisition time and high sensitivity to haemorrhage.[16] This technique is commonly used in combination with DWI, especially for subjects with suspected acute neurologic abnormalities.[17] In addition to haemorrhage evaluation, the venous oxygen content can be approximated by T2* imaging, particularly its phase information.[18] If cerebral oxygen extraction or utilization is impaired, then the oxygenation status of venous blood will also be altered and show a distinct T2* signature that can be easily differentiated from venous blood with a normal oxygenation status on GRE-based images.[12,13]

In the present study, we used phase images of T2*WI as surrogate markers of abnormal cerebral venous oxygenation in CA survivors. The purpose of this study was to investigate the prognostic value of phase information from T2*WI in these patients by identifying abnormal brain oxygen extraction. In addition, we investigated the clinical aspect of phase information using correlations with previously suggested biomarkers of brain damage and electroencephalography.

Methods

Study protocol and subjects

This retrospective, observational study using prospectively collected data was conducted in a single tertiary hospital in Seoul, Korea. The study consisted of two phases: a preliminary study and the actual study. The preliminary study aimed to define normal findings for venous structures on T2*WI. From June to July 2016, a convenience sample of 10 patients without anoxia–ischaemia who underwent the same T2*WI protocol was examined. We found clear, consistently high phase values for three venous structures (the superior sagittal sinus [SSS], cortical veins [CV], and thalamostriate veins [TV], Fig. 1) on filtered phase images of T2*WI (the processing methods are described in the following paragraph). High phase values of cerebral venous structures reflected a substantial amount of paramagnetic deoxyhaemoglobin in venous blood from normal cerebral oxygen metabolism. Therefore, we hypothesized that deviation of venous contrast from this pattern can be indicative of abnormal oxygen metabolism in the brain. The SSS, CV and TV were used as representative venous structures in the following evaluation.

For the actual study, we identified adult ($\geq$ 18 years of age) CA survivors who underwent MRI for prognostication from a prospectively collected TH registry between June 2016 and April 2018. The exclusion criteria included unavailable phase data of T2*WI, transferred patients and an excessive interval between CA and MRI scanning (>120 h). This study was approved by our Institutional Review Board, which waived the requirement for informed consent because of the noninterventional, retrospective nature of this study.

Post-CA care protocols

During the study period, all comatose patients with return of spontaneous circulation (ROSC) were considered eligible for TH at 33 °C for 24 h. Details of standard TH are provided in the Supplementary Methods.

Continuous amplitude-integrated electroencephalography (aEEG) using a multichannel device (Xltek EEG32U, Natus, Inc., Seattle, WA, USA) or a single-channel device (Olympic Brain Monitor, Natus, Inc., Seattle, WA, USA) was performed on all patients in the emergency department or intensive care unit.[1] Recording continued until the patient regained consciousness, the patient died, or at least 72 h had passed since ROSC. As a surrogate marker for neuronal injury, measurements of neuron-specific enolase (NSE) and S100 calcium-binding protein B (S100B) were obtained as soon as possible after ROSC, and these measurements were repeated 24, 48, and 72 h later.

After completion of TH, MRI was performed as a part of the standard prediction protocol (Supplementary Methods). The treatment team provided sufficiently prolonged life support to patients who did not recover consciousness before discharge to a long-term care facility.

Outcome measurements

The primary outcome of this study was a poor neurological outcome, which was categorized according to the Cerebral Performance Categories (CPCs) at 6 months after CA. Outcomes were dichotomized into good (CPCs 1 and 2) and poor (CPCs 3–5) outcomes.

Processing and evaluation of T2*WI phase images

We used the appearance of three venous structures on phase images as imaging surrogates of cerebral oxygen metabolism. To enhance the reliability of the phase contrast of venous structures on T2*WI phase images, we applied homodyne filtering to remove the unwanted background phase mainly induced by air/tissue boundaries or system imperfections.[19] Two investigators (JJ and SHO) blindly reviewed venous structures on filtered phase images without patient information to reach a consensus. Based on the normal appearance of venous structures from a preliminary study, the phase contrast of these venous structures was sorted into two categories: normal (score 0) and abnormal (score 1). A standard window setting (width 16,000 rad/s, centre 0 rad/s) was used for visual analysis; this setting was empirically selected to demonstrate good venous contrast in control subjects. Inter-observer reliability before a consensus was reached was good to excellent (Supplementary Methods). The summary GRE score of each subject was calculated after the sum of three venous scores. Patterns of abnormal phase contrast were reclassified as increased (high) or decreased (low) contrast of venous structures (Fig. 1). For quantitative measures, a manual region of interest (ROI) was drawn for the SSS to measure the phase value. Two other venous structures were not used because they were too small for ROI placement or partial volume averaging. An oval ROI > 15 mm^2 was

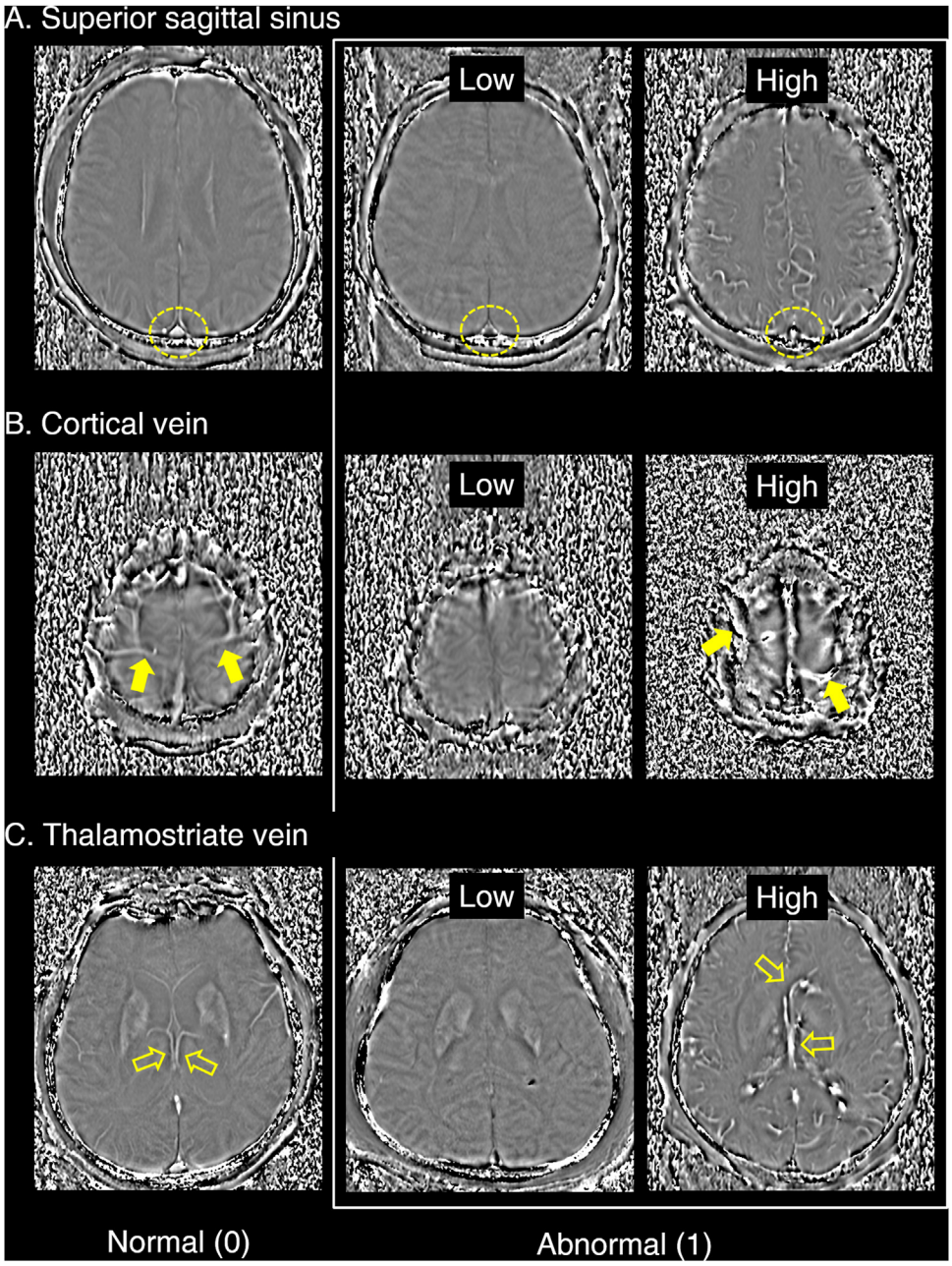

Fig. 1 – Normal and abnormal findings of venous structures on filtered phase images.
Filtered phase images of T2*-weighted GRE showed good contrast of venous structures. The three representative venous structures used in this study were the superior sagittal sinus (A, dashed circle), cortical veins (B, solid arrow) and thalamostriate veins (C, open arrow). Note the clear and bright contrast of those venous structures under normal conditions (left column, score 0). Patients with abnormal venous contrast (score 1) showed either decreased (low, middle column) or accentuated contrast (high, right column) compared with the normal state.

placed at the posterior aspect of the SSS, and the mean phase value of the SSS was obtained.

Known predictors of a poor outcome

Assessment of DWI was performed using the following categories: (1) no DWI lesion, (2) (multi) focal DWI lesions sparing the basal ganglia (BG), (3) (multi) focal DWI lesions including the BG, and (4) diffuse diffusion-restricted lesions of the brain.[20] The last aEEG background patterns were simply classified into the following three categories using the voltage method: continuous normal voltage (CNV), others, and a flat trace.[1] Regarding biomarkers, the highest serum values of NSE and S100B at 48 and 72 h after ROSC were used as surrogate markers.[19] Serum was analysed with Roche Elecsys NSE and S100 reagents (Roche Diagnostics, Mannheim, Germany). If the serum showed significant haemolysis, the results were discarded.

Statistical analysis

DWI findings, visual scores of filtered phase images, the mean phase value of the SSS, aEEG categories and biomarkers were compared between the good and poor outcome groups using a t-test, Mann-Whitney U test, chi-squared test or Fisher's exact test. Prognostic performance was evaluated using a receiver operating characteristic (ROC) curve. We also created combined models using logistic regression models. Comparison of the area under the curve (AUC) of the ROC curves was performed using DeLong's test.[21] Additionally, clinical and imaging characteristics were compared according to GRE summary scores. All analyses were performed with the R statistical package (version 3.4.4, R Foundation, Vienna, Austria; www.R-project.org). A *P* value of 0.05 or smaller was considered statistically significant for all statistical analyses.

Results

Characteristics of the participants

During the study period, 43 survivors of CA underwent MRI for prognostication. Among them, 4 patients were excluded because of loss of T2*WI phase data (n = 1), use of a different scanning protocol (n = 1), different (outside) post-CA treatment (n = 1), or delayed MRI scan (n = 1). Finally, 39 patients were included in this study. Among them, 12 patients (31%) had good outcomes, and 27 patients (69%) had poor outcomes. The baseline characteristics of the participants and the results of known prognostic markers are summarized in Table 1.

Prognostic value of phase images of T2*WI

The scores for three venous structures and the summary GRE score of the poor outcome group were significantly higher than those of the good outcome group (Table 2). In particular, all patients with a good outcome showed normal phase contrast for the SSS, and only one patient with a poor outcome (1/27, 3.7%) had a normal SSS phase pattern. The AUC for prediction of a poor outcome was calculated to evaluate the predictive value of each predictor (Fig. 2). ROC curve analysis showed good performance for prognostication of T2*WI. The AUCs of the GRE summary score and mean phase value of the SSS (AUCs 0.980 and 0.920, respectively) were comparable to those of conventional outcome predictors, including DWI patterns (AUC 0.949), with no statistically significant difference (all *P* values > 0.05, data not shown). The AUC of the logistic regression models with combinations of summary GRE scores added to DWI patterns was calculated. Compared to a single predictive factor, the AUC increased when the summary GRE score was added to DWI patterns (AUC 0.991), although the difference was not statistically significant ($P = 0.117$). Representative cases are presented in Supplementary Figs. 1–4.

Associations of other outcome predictors with phase image findings

Table 3 shows the results of other outcome predictors according to GRE scores. DWI patterns, aEEG, and serum biomarkers levels were significantly different according to GRE scores. Generally, GRE scores were associated with other outcome predictors, including DWI patterns. However, some discrepancies were noted between GRE scores and DWI patterns. Among 13 patients with normal DWI, four patients had a GRE score of 2. Two of these patients (2/4) were discharged with poor outcomes (Supplementary Fig. 1). On the other hand, all subjects with a GRE score of 0 (normal contrast in all three venous structures) had a good outcome (n = 9), and all of them showed normal aEEG patterns. All subjects with a GRE score of 3 (abnormal contrast in all three venous structures) had poor outcomes

Table 1 – Characteristics of included subjects.

	Good outcome (n = 12)	Poor outcome (n = 27)	*P* value
Age, mean (SD), years	49.7 (18.8)	53.4 (16.7)	0.542
Male	4 (33.3)	11 (40.7)	0.834
CPC at discharge			
1	11 (91.7)	0 (0.0)	<0.001
2	1 (8.3)	0 (0.0)	
3	0 (0.0)	2 (7.4)	
4	0 (0.0)	9 (33.3)	
5	0 (0.0)	16 (59.3)	
Interval between cardiac arrest and MRI scan, mean (SD), hours	76.7 (19.8)	73.6 (14.9)	0.587
DWI lesions			
No DWI lesion	11 (91.7)	2 (7.4)	<0.001
Focal DWI lesions sparing BG	1 (8.3)	7 (25.9)	
Focal DWI lesions including BG	0 (0.0)	1 (3.7)	
Diffuse DWI lesions	0 (0%)	17 (63.0)	
S100B, median (IQR), ng/mL[a]	0.10 (0.08, 0.15)	0.53 (0.23, 2.90)	<0.001
NSE, median (IQR), ng/mL[a]	21.68 (18.10, 31.39)	90.84 (47.56, 153.22)	<0.001
aEEG patterns			
CNV	12 (100.0)	4 (14.8)	<0.001
Others	0 (0.0)	17 (63.0)	
Flat trace	0 (0.0)	6 (22.2)	

CPC, Cerebral Performance Category; MRI, magnetic resonance imaging; DWI, diffusion-weighted images; BG, basal ganglia; S100B, S100 calcium-binding protein B; NSE, neuron-specific enolase; aEEG, amplitude integrated electroencephalography; CNV, continuous normal voltage.

[a] Highest serum values during 48 and 72 h after return of spontaneous circulation. One subject did not have an s100B or NSE value due to clinical circumstances.

Table 2 – Filtered phase image assessment results.

	Good outcome (n = 12)	Poor outcome (n = 27)	*P* value
Patterns of three venous structures (scores)			
SSS			
Normal (0)	12 (100.0)	1 (3.7)	<0.001
Abnormal – low (1)	0 (0.0)	24 (88.9)	
Abnormal – high (1)	0 (0.0)	2 (7.4)	
CV			
Normal (0)	9 (75.0)	0 (0.0)	<0.001
Abnormal – low (1)	3 (25.0)	22 (81.5)	
Abnormal – high (1)	0 (0.0)	5 (18.5)	
TV			
Normal (0)	10 (83.3)	5 (18.5)	0.001
Abnormal – low (1)	2 (16.7)	17 (63.0)	
Abnormal – high (1)	0 (0.0)	5 (18.5)	
Summary GRE score			
0	9 (75.0)	0 (0)	<0.001
1	1 (8.3)	1 (3.7)	
2	2 (16.7)	4 (14.8)	
3	0 (0.0)	22 (81.5)	
Phase value of ROI at SSS, mean (SD), rad/s	0.39 (0.14)	0.10 (0.57)	0.019
Standard deviation of phase value of ROI, mean (SD), rad/s	0.27 (0.15)	0.30 (0.26)	0.722
ROI size, mean (SD), mm^2	74.5 (27.1)	77.7 (26.6)	0.728

SSS, superior sagittal sinus; CV, cortical vein; TV, thalamostriate vein; GRE, gradient echo image; ROI, region of interest.

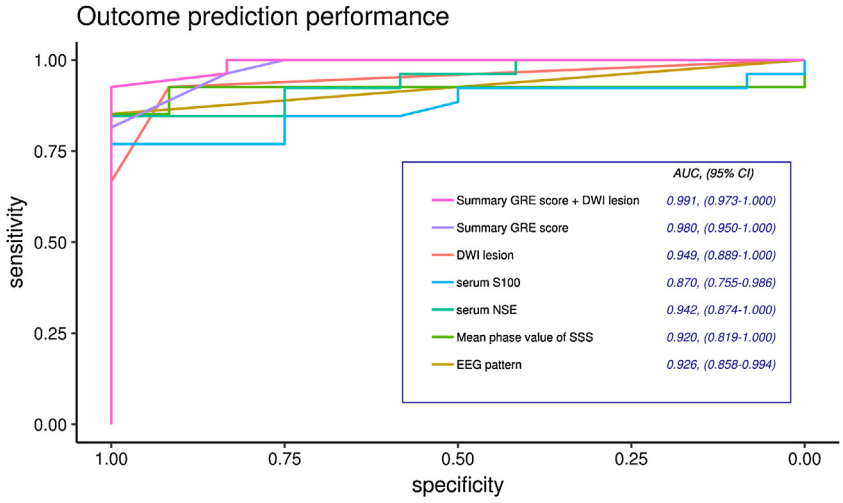

Fig. 2 – Outcome prediction performances for cardiac arrest survivors.
The receiver operating characteristic curves showed good prognosis prediction performance for summary GRE scores and mean phase values of SSS, as well as known prognostic markers. Note that the combination of summary GRE score and DWI lesion has the highest AUC.
AUC, area under the curve; CI, confidence interval.

(n = 22), but they also showed variable DWI patterns (diffuse lesions, n = 15; focal lesions including the BG, n = 1; and focal lesions sparing the BG, n = 6, Supplementary Figs. 2 and 3).

All subjects with flat traces on aEEG showed a high GRE score of 3 (6/6), and 5 of these patients showed an abnormal phase of high contrast in venous structures (2 of SSS, 5 of CV, 5 of TV). Among the 5 patients with high contrast in cerebral venous structures on filtered phase images of T2*WI, four (4/5, 80%, Supplementary Fig. 3) were diagnosed with brain death and underwent organ donation.

Discussion

This study demonstrated the prognostic value of phase images of T2*WI in CA survivors. The performances of GRE scores and the mean phase value of the SSS for prognostication were comparable to those of previously reported prognostic markers, including DWI patterns, biomarkers and aEEG. When the summary GRE score is added to DWI patterns, the prognostic value of MRI may be improved.

Table 3 – Relationship between GRE score and other prognostic markers.

	GRE score				*P* value
	0 (n = 9)	1 (n = 2)	2 (n = 6)	3 (n = 22)	
Age, mean (SD), years	46.89 (20.65)	46.50 (20.51)	55.50 (14.10)	54.05 (16.88)	0.274
Male	5 (55.6)	2 (100.0)	3 (50.0)	14 (63.6)	0.623
Outcome					
Good	9 (100.0)	1 (50.0)	2 (33.3)	0 (0.0)	<0.001
Poor	0 (0.0)	1 (50.0)	4 (66.7)	22 (100.0)	
DWI findings					
Normal	8 (88.9)	1 (50.0)	4 (66.6)	0 (0.0)	0.001
Focal sparing basal ganglia	1 (11.1)	0 (0.0)	1 (16.7)	6 (27.3)	
Focal including basal ganglia	0 (0.0)	0 (0.0)	0 (0.0)	1 (4.5)	
Diffuse	0 (0.0)	1 (50.0)	1 (16.7)	15 (68.2)	
aEEG findings					
CNV	9 (100.0)	1 (50.0)	3 (50.0)	3 (13.6)	0.001
Others	0 (0.0)	1 (50.0)	3 (50.0)	13 (59.1)	
Flat trace	0 (0.0)	0 (0.0)	0 (0.0)	6 (27.3)	
Phase value of ROI, median (IQR), rad/s	0.33 (0.28, 0.48)	0.34 (0.24, 0.44)	0.21 (0.15, 0.25)	0.02 (−0.08, 0.05)	<0.001
S100B, median (IQR), ng/mL[a]	0.10 (0.08, 0.13)	0.20 (0.10, 0.30)	0.23 (0.17, 0.34)	1.01 (0.23, 5.19)	0.003
NSE median (IQR), ng/mL[a]	20.70 (17.56, 25.04)	50.00 (20.18, 79.83)	31.39 (23.06, 71.81)	104.50 (50.94, 153.22)	<0.001

GRE, gradient echo image; DWI, diffusion-weighted images; aEEG, amplitude integrated electroencephalography; CNV, continuous normal voltage; ROI, region of interest; S100B, S100 calcium-binding protein B; NSE, neuron-specific enolase.
[a] Highest serum values during 48 and 72 h after return of spontaneous circulation. One subject did not have an s100B or NSE value due to clinical circumstances.

Patients with poor outcomes showed high summary GRE scores, which suggested abnormal cerebral oxygen extraction as demonstrated by abnormal contrast on filtered phase images of T2*WI. This abnormal contrast is due to an altered venous concentration of deoxyhaemoglobin. In contrast, most patients with good outcomes showed normal contrast of cerebral venous structures, suggesting the possibility of a relatively preserved oxygen extraction fraction (OEF) and possibly cerebral oxygen metabolism.

Several previous studies have reported decreased oxygen metabolism in the brains of CA survivors.[5–9] Regarding the prognostic value of cerebral oxygen metabolism, compared with control groups, these studies suggested that decreased cerebral oxygen metabolism was more pronounced in patients with poor outcomes, while the OEF was modestly decreased in subjects with good outcomes.[5,7,9] Our result is consistent with this finding; most patients with poor outcomes showed decreased phase contrast of venous structures, suggesting decreased cerebral oxygen metabolism. Previous studies have suggested persistently decreased oxygen metabolism in CA survivors despite restoration of cerebral blood flow (CBF).[5,7] One possible explanation is decreased neuronal activity after CA.[7,22] In addition, direct brain damage due to hypoxic-ischaemic injury may decrease oxygen metabolism in the brain.[3,23] These findings supported that the prognostic value of cerebral venous oxygenation status and their surrogate imaging techniques were based on their association with functional and physical damage to neurons.

In the present study, we found some discrepancies between DWI patterns and GRE scores. T2*WI in patients with a GRE score of 3 presented variable DWI findings. Additionally, normal DWI patterns were not a guarantee for a good outcome. Interestingly, some cases (2/11) showed abnormal GRE scores and had poor outcomes. Although statistically underpowered, this pilot study suggested that a combination of findings on DWI and filtered phase images of T2*WI may be useful for prognostication of CA survivors. A previous report suggested different patterns of metabolic and functional recovery after CA in an animal model,[22] which suggested correlated but not identical findings for each prognostic marker. Based on this evidence, current recommendations suggest the use of a multimodal approach to predict outcomes.[24,25] A single prognostic tool may be limited for detailed prognostication because each tool has a unique background as a method to estimate neuronal damage in CA survivors. For example, DWI visualizes the degree and extent of hypoxic-ischaemic brain injuries, particularly those showing cytotoxic oedema.[3,26] The electrocortical background activity provides information on the level of brain activity.[27]

All subjects with a normal T2*WI showed a normal aEEG pattern. These results suggested that normal GRE venous patterns may indicate preserved neuronal activity.[1] Additionally, 5 of 6 subjects with flat-trace aEEG patterns showed abnormally increased phase contrast. These findings are similar to reported findings on susceptibility-weighted images of brain death.[28] Additionally, these subjects showed findings of brain oedema on conventional brain MR images, including collapsed cisterns and ventricles. Despite the decreased neuronal activity of CA survivors and brain death subjects,[7,22] markedly increased intracranial pressure may have induced a substantially increased OEF via decreased cerebral perfusion pressure and subsequently prolonged cerebral blood transit time.[28] Evaluation of T2*WI may facilitate the decision to apply a diagnostic protocol for brain death. From this perspective, phase images of T2*WI may have potential as a convenient prognostication battery. Our findings suggested that we can identify a subgroup of subjects with a poor prognosis — brain death — using phase images of T2*WI.

Although assessing internal jugular venous oxygenation is a common approach for cerebral oxygenation status evaluation,[29] we used routine clinical T2*WI for this purpose. One important benefit of phase information of T2*WI is that it can be acquired from current, widely used, simple and fast MR protocols. T2*WI is available in all clinical MR machines and is accepted as a routine clinical practice for MR imaging in various neurological diseases.[16] Additionally, imaging CA survivors with complex and delicate pulse sequences[10,11] may be challenging because of frequently accompanying clinical factors, such as mechanical ventilation

and unstable vital signs. Another benefit of T2*WI is the very short acquisition time (less than 1 min), which is helpful for improving the clinical compliance of patients. Our results suggested the clinical usefulness of phase information of T2*WI in this challenging condition as a simplified tool for cerebral venous oxygenation assessment.

However, protocols for cerebral oxygen metabolism assessment using MRI can be further optimized. For example, our approach was limited in its ability to conduct a detailed assessment of cerebral venous oxygen status with respect to regional information and quantitative parameters. Venous blood in the SSS may be contaminated by diploic veins from the scalp, and better clinical information can be obtained from deep venous structures. Although we assessed deep venous structures qualitatively, detailed evaluations of these structures were limited due to slice thickness and the interslice gap. Optimized protocols may yield rich quantitative measurements of cerebral venous oxygen status. Additional assessment of CBF and volume may estimate the cerebral metabolic rate of oxygen in addition to OEF surrogates.[10,12,13] Such protocols may also provide an improved, detailed understanding of oxygen metabolism in the brains of CA survivors and increase its clinical value.

This study has several limitations. First, although we performed this study using consecutive subjects, the relatively small number of subjects and the retrospective nature of this study may introduce some bias, including a selection bias. This limitation may restrict the generalization of our results; thus, larger, prospective studies are warranted. Second, we did not perform a follow-up or serial observations of MR data, and we did not observe dynamic changes in cerebral venous oxygenation status in the subjects. Although we used phase images as a surrogate of the OEF, we did not estimate the exact CBF or the cerebral metabolic rate of oxygen. As discussed earlier, we used phase information of T2*WI, which may be optimized for magnitude images. Further work is required to optimize protocols for CA survivors.

Conclusions

Filtered phase images from T2*WI may be a valuable imaging tool to predict neurological outcomes after CA and showed prognostic value comparable to that of other outcome predictors. This tool can reveal various features of cerebral oxygen metabolic consequences after CA that are associated with a poor outcome, such as decreased neuronal activity or brain death-like patterns. Filtered phase images of T2*WI in these patients may improve neurological outcome prediction as one method of multimodal approach.

Acknowledgements

This work was supported by a National Research Foundation of Korea grant funded by the Korean government (MSIT) (No. NRF-2016R1C1B1009088) and the Ministry of Education (NRF-2017R1D1A1B03033829). We thank the Cerebral Resuscitation and Outcome evaluation Within catholic Network (CROWN) investigators for contributing to data collection.

Conflict of Interest

None

Appendix A. Supplementary data

Supplementary material related to this article can be found, in the online version, at doi:https://doi.org/10.1016/j.resuscitation.2019.05.026.

REFERENCES

1. Oh SH, Park KN, Shon YM, et al. Continuous amplitude-integrated electroencephalographic monitoring is a useful prognostic tool for hypothermia-treated cardiac arrest patients. Circulation 2015;132:1094–103.
2. Karapetkova M, Koenig MA, Jia X. Early prognostication markers in cardiac arrest patients treated with hypothermia. Eur J Neurol 2016;23:476–88.
3. Wu O, Sorensen AG, Benner T, Singhal AB, Furie KL, Greer DM. Comatose patients with cardiac arrest: predicting clinical outcome with diffusion-weighted MR imaging. Radiology 2009;252:173–81.
4. Wijman CA, Mlynash M, Caulfield AF, et al. Prognostic value of brain diffusion-weighted imaging after cardiac arrest. Ann Neurol 2009;65:394–402.
5. Edgren E, Enblad P, Grenvik Å, et al. Cerebral blood flow and metabolism after cardiopulmonary resuscitation. A pathophysiologic and prognostic positron emission tomography pilot study. Resuscitation 2003;57:161–70.
6. Ahn A, Nasir A, Malik H, D'Orazi F, Parnia S. A pilot study examining the role of regional cerebral oxygen saturation monitoring as a marker of return of spontaneous circulation in shockable (VF/VT) and non-shockable (pea/asystole) causes of cardiac arrest. Resuscitation 2013;84:1713–6.
7. Hoedemaekers CW, Ainslie PN, Hinssen S, et al. Low cerebral blood flow after cardiac arrest is not associated with anaerobic cerebral metabolism. Resuscitation 2017;120:45–50.
8. Putzer G, Braun P, Strapazzon G, et al. Monitoring of brain oxygenation during hypothermic CPR — a prospective porcine study. Resuscitation 2016;104:1–5.
9. Mortberg E, Cumming P, Wiklund L, Rubertsson S. Cerebral metabolic rate of oxygen (cmro2) in pig brain determined by pet after resuscitation from cardiac arrest. Resuscitation 2009;80:701–6.
10. Rodgers ZB, Leinwand SE, Keenan BT, Kini LG, Schwab RJ, Wehrli FW. Cerebral metabolic rate of oxygen in obstructive sleep apnea at rest and in response to breath-hold challenge. J Cereb Blood Flow Metab 2016;36:755–67.
11. Uwano I, Kudo K, Sato R, et al. Noninvasive assessment of oxygen extraction fraction in chronic ischemia using quantitative susceptibility mapping at 7 tesla. Stroke 2017;48:2136–41.
12. Kudo K, Liu T, Murakami T, et al. Oxygen extraction fraction measurement using quantitative susceptibility mapping: comparison with positron emission tomography. J Cereb Blood Flow Metab 2016;36:1424–33.
13. Wehrli FW, Fan AP, Rodgers ZB, Englund EK, Langham MC. Susceptibility-based time-resolved whole-organ and regional tissue oximetry. NMR Biomed 201730:.
14. Rodgers ZB, Detre JA, Wehrli FW. MRI-based methods for quantification of the cerebral metabolic rate of oxygen. J Cereb Blood Flow Metab 2016;36:1165–85.
15. Zhang J, Liu T, Gupta A, Spincemaille P, Nguyen TD, Wang Y. Quantitative mapping of cerebral metabolic rate of oxygen (CMRO2) using quantitative susceptibility mapping (QSM). Magn Reson Med 2015;74:945–52.
16. Markl M, Leupold J. Gradient echo imaging. J Magn Reson Imaging 2012;35:1274–89.
17. Wintermark M, Sanelli PC, Albers GW, et al. Imaging recommendations for acute stroke and transient ischemic attack patients: a joint statement by the American Society of Neuroradiology, the American College of Radiology, and the Society of Neurointerventional Surgery. AJNR Am J Neuroradiol 2013;34:E117–27.

18. Liu C, Li W, Tong KA, Yeom KW, Kuzminski S. Susceptibility-weighted imaging and quantitative susceptibility mapping in the brain. J Magn Reson Imaging 2015;42:23–41.
19. Haacke EM, Xu Y, Cheng YC, Reichenbach JR. Susceptibility weighted imaging (SWI). Magn Reson Med 2004;52:612–8.
20. Sandroni C, Cavallaro F, Callaway CW, et al. Predictors of poor neurological outcome in adult comatose survivors of cardiac arrest: A systematic review and meta-analysis. Part 2: Patients treated with therapeutic hypothermia. Resuscitation 2013;84:1324–38.
21. Robin X, Turck N, Hainard A, et al. pROC: An open-source package for R and S+ to analyze and compare ROC curves. BMC Bioinf 2011;12:77.
22. Bernd S, Mathias HB, KC M, BB W, Konstantin-Alexander H. Recovery of the rodent brain after cardiac arrest: A functional mri study. Magn Reson Med 1998;39:783–8.
23. Mlynash M, Campbell DM, Leproust EM, et al. Temporal and spatial profile of brain diffusion-weighted MRI after cardiac arrest. Stroke 2010;41:1665–72.
24. Sandroni C, Cariou A, Cavallaro F, et al. Prognostication in comatose survivors of cardiac arrest: an advisory statement from the European Resuscitation Council and the European Society of Intensive Care Medicine. Resuscitation 2014;85:1779–89.
25. Callaway CW, Donnino MW, Fink EL, et al. Part 8: Post-cardiac arrest care: 2015 American Heart Association guidelines update for cardiopulmonary resuscitation and emergency cardiovascular care. Circulation 2015;132:S465–82.
26. Moon HK, Jang J, Park KN, et al. Quantitative analysis of relative volume of low apparent diffusion coefficient value can predict neurologic outcome after cardiac arrest. Resuscitation 2018;126:36–42.
27. Hellstrom-Westas L, Rosen I. Continuous brain-function monitoring: state of the art in clinical practice. Semin Fetal Neonatal Med 2006;11:503–11.
28. Sohn CH, Lee HP, Park JB, et al. Imaging findings of brain death on 3-tesla MRI. Korean J Radiol 2012;13:541–9.
29. Buunk G, van der Hoeven JG, Meinders AE. Prognostic significance of the difference between mixed venous and jugular bulb oxygen saturation in comatose patients resuscitated from a cardiac arrest. Resuscitation 1999;41:257–62.